

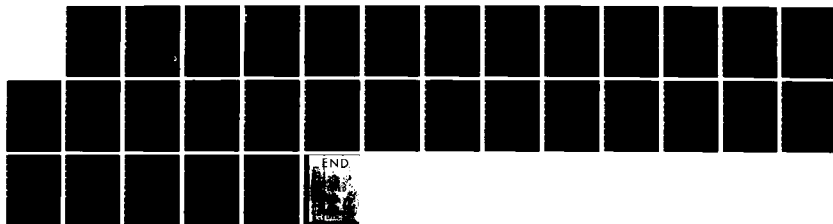
AD-A136 607

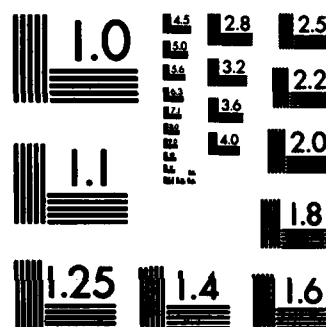
OPTICAL SCINTILLATION STATISTICS FOR INFRARED
GROUND-TO-SPACE LASER COMMU. (U) AEROSPACE CORP EL
SEGUNDO CA ELECTRONICS RESEARCH LAB H T YURA ET AL.
01 DEC 83 TR-0084(4925-04)-1 SD-TR-83-80 F/G 17/2

1/1

UNCLASSIFIED

NL





MICROCOPY RESOLUTION TEST CHART
NATIONAL BUREAU OF STANDARDS-1963-A

12

AD-A136607

Space System Statistics
Space System Statistics
Space System Statistics

DTIC
ELECTE
S D
JAN 06 1964
E

DTIC FILE COPY

Prepared for
SPACE DIVISION
AIR FORCE SYSTEMS COMMAND
Los Angeles Air Force Station
P.O. Box 92960, Worldway Postal Center
Los Angeles, Calif. 90009

84 01 06 016

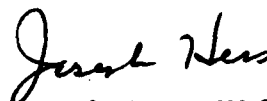
This report was submitted by The Aerospace Corporation, El Segundo, CA 90245, under Contract No. F04701-83-C-0084 with the Space Division, P.O. Box 92960, Worldway Postal Center, Los Angeles, CA 90009. It was reviewed and approved for The Aerospace Corporation by D. H. Phillips, Director, Electronics Research Laboratory. 1st Lt. Lawrence J. Zappone, SD/YKXL, was the project officer for the Mission-Oriented Investigation and Experimentation (MOIE) Program.

This report has been reviewed by the Public Affairs Office (PAS) and is releasable to the National Technical Information Service (NTIS). At NTIS, it will be available to the general public, including foreign nationals.

This technical report has been reviewed and is approved for publication. Publication of this report does not constitute Air Force approval of the report's findings or conclusions. It is published only for the exchange and stimulation of ideas.



Lawrence J. Zappone, 1st Lt, USAF
Project Officer



Joseph Hess, GM-15, Director
West Coast Office, AF Space
Technology Center

UNCLASSIFIED

SECURITY CLASSIFICATION OF THIS PAGE (When Data Entered)

REPORT DOCUMENTATION PAGE		READ INSTRUCTIONS BEFORE COMPLETING FORM
1. REPORT NUMBER SD-TR-83-80	2. GOVT ACCESSION NO. AD-A136 607	3. RECIPIENT'S CATALOG NUMBER
4. TITLE (and Subtitle) OPTICAL SCINTILLATION STATISTICS FOR INFRARED GROUND-TO-SPACE LASER COMMUNICATION SYSTEMS		5. TYPE OF REPORT & PERIOD COVERED
		6. PERFORMING ORG. REPORT NUMBER TR-0084(4925-04)-1
7. AUTHOR(s) Hal T. Yura and W. G. McKinley		8. CONTRACT OR GRANT NUMBER(s) F04701-83-C-0084
9. PERFORMING ORGANIZATION NAME AND ADDRESS The Aerospace Corporation El Segundo, Calif. 90245		10. PROGRAM ELEMENT, PROJECT, TASK AREA & WORK UNIT NUMBERS
11. CONTROLLING OFFICE NAME AND ADDRESS Space Division Los Angeles Air Force Station Los Angeles, Calif. 90009		12. REPORT DATE 1 December 1983
		13. NUMBER OF PAGES 31
14. MONITORING AGENCY NAME & ADDRESS (if different from Controlling Office)		15. SECURITY CLASS. (of this report) Unclassified
		15a. DECLASSIFICATION/DOWNGRADING SCHEDULE
16. DISTRIBUTION STATEMENT (of this Report) Approved for public release; distribution unlimited		
17. DISTRIBUTION STATEMENT (of the abstract entered in Block 20, if different from Report)		
18. SUPPLEMENTARY NOTES		
19. KEY WORDS (Continue on reverse side if necessary and identify by block number) Atmospheric Turbulence Laser Communications Scintillation		
20. ABSTRACT (Continue on reverse side if necessary and identify by block number) Statistical estimates of selected scintillation parameters for an infrared laser ground-to-space communication system are presented for a point receiving aperture. The quantities estimated here are the fraction of time that the signal power is both above and below a given value, the mean number of times per second the signal power crosses a given signal level, and the mean duration of both surges and fades for a given log-irradiance variance.		

CONTENTS

I. INTRODUCTION.....	7
II. SPATIAL STATISTICS.....	8
III. TEMPORAL STATISTICS.....	14
IV. FADE AND SURGE STATISTICS.....	17
A. Fraction of Time of Fades and Surges.....	18
B. Mean Frequency of Level Crossings.....	19
C. Mean Duration of Fades and Surges.....	27
V. DISCUSSION.....	27
REFERENCES.....	31

Accession For	
NTIS GRA&I	<input checked="" type="checkbox"/>
DTIC TAB	<input type="checkbox"/>
Unannounced	<input type="checkbox"/>
Justification	
By	
Distribution/	
Availability Codes	
Dist	Avail and/or Special
A-1	



TABLE

1.	Log-Irradiance Variance at Several Wavelengths for Various Values of the Root-Mean-Square Wind Speed and Zenith Angles.....	13
----	---	----

FIGURES

1.	Normalized Log-Irradiance Variance as a Function of Root-Mean-Square Wind Speed V	12
2.	Normalized Irradiance Temporal Frequency Spectrum for Various Values of V at $\lambda = 2.91 \mu\text{m}$	16
3.	Fraction of Time that the Irradiance is Less than 3, 6, and 10 dB Below the Mean Intensity.....	20
4.	Fraction of Time that the Irradiance is Greater than 3 and 6 dB Above the Mean Intensity Level.....	21
5.	Mean Level Crossing Frequency as a Function of Normalized Log-Irradiance Variance for Various Fade Levels, $\lambda = 2.91 \mu\text{m}$	23
6.	Mean Level Crossing Frequency as a Function of Fade Level for Various Wavelengths: $V = 36 \text{ m/s}$, $\theta = 0^\circ$	24
7.	Mean Level Crossing Frequency as a Function of Fade Level for Various Wavelengths: $V = 36 \text{ m/s}$, $\theta = 60^\circ$	25
8.	Mean Level Crossing Frequency at $\lambda = 1.32 \mu\text{m}$ for Various Root-Mean-Square Wind Speeds and Zenith Angles.....	26
9.	Mean Duration of 3 and 6 dB Fades as a Function of Normalized Log-Irradiance Variance.....	28

I. INTRODUCTION

For a number of electro-optical system applications (e.g., laser communications) it is desirable to have available quantitative estimates of various statistical quantities that are associated with atmospheric turbulence-induced irradiance fluctuations (i.e., scintillation). To this end, we have calculated the magnitude, temporal power spectrum, and fade/surge statistics for the optical scintillation of a monochromatic ground-based laser source operating in the 1 to 10 μ m wavelength region, as observed by a small receiving aperture at an exo-atmospheric location.

As indicated below, scintillation effects are primarily the result of high-altitude clear air turbulence. For ground-to-space applications one must employ an appropriate index structure constant profile model in order to obtain numerical results. Although a number of C_n^2 models exist in the literature, we will apply one developed by Hufnagel.⁽¹⁾ In addition to being mathematically convenient, this C_n^2 model provides fairly good agreement between the observed and predicted values of the log-amplitude variance of irradiance from stellar sources. Furthermore, as discussed below, Hufnagel's model agrees fairly well with measured values of C_n^2 profiles (e.g., see Table VII - IX of Ref. 2). In any event, although the numerical results presented here are based on the Hufnagel model, the analytic expressions presented below are valid for an arbitrary C_n^2 profile. This turbulence model contains one independent parameter, the root-mean-square wind speed V between altitudes of 5 and 20 km above mean sea level, i.e.,

$$V = \left[\frac{1}{15} \int_5^{20} v^2(h) dh \right]^{1/2}.$$

The quantity V can be obtained, for example, from rawinsonde data and is typically in the 20 - 35 m/s range. In Ref. 1, Hufnagel comments that, for the State of Maryland, V is normally distributed about 27 m/s with a standard deviation of 9 m/s. Furthermore, for ground-to-space propagation conditions the characteristic irradiance correlation length at the location of the receiver is typically much larger than the diameter of the receiving aperture. As such, we can assume that the receiver is a "point-receiver" and thus no aperture averaging effects are expected.

II. SPATIAL STATISTICS

For all cases of interest here, the variance of irradiance when normalized by the mean irradiance level is much less than unity. Therefore, the log irradiance l is normally distributed. It is operationally useful to define the log-irradiance l by

$$l(r, t) = \frac{I(\underline{r}, t)}{I_m} \equiv e^l, \quad (1)$$

where $I(\underline{r}, t)$ is the irradiance at position vector \underline{r} and time t , and I_m is its mean value. If the variance of l is small compared to unity, the probability distribution for l is normal, (2)

$$P_l(l) = \frac{1}{(2\pi\sigma_l^2)^{1/2}} \exp\left[-\frac{(l - l_m)^2}{2\sigma_l^2}\right], \quad (2)$$

where l_m is the mean value of l , and

$$\sigma_l^2 = \langle (l - l_m)^2 \rangle = \langle [\ln(I/I_m)]^2 \rangle. \quad (3)$$

Also, it can be shown that $\ell_m = \langle \ell \rangle = -(1/2)\sigma_\ell^2$. Then, the probability distribution for log irradiance is characterized by one quantity, σ_ℓ^2 , the variance of log irradiance:

$$P_\ell(\ell) = \frac{1}{(2\pi\sigma_\ell^2)^{1/2}} \exp\left\{-\frac{[\ell + (1/2)\sigma_\ell^2]^2}{2\sigma_\ell^2}\right\}. \quad (4)$$

It follows that the distribution function for $P_1(i)$ is log normal and is given by

$$P_1(i) = \frac{1}{(2\pi\sigma_\ell^2)^{1/2}} \frac{1}{i} \exp\left\{-\frac{1}{2\sigma_\ell^2} \left[\ln i + \frac{1}{2}\sigma_\ell^2\right]^2\right\}. \quad (5)$$

While σ_ℓ^2 , the variance of log-irradiance, appears in the literature as the most common measure of the magnitude of scintillation, it can be simply related to the normalized irradiance variance as

$$\sigma_I^2 \equiv \frac{\langle (I - I_m)^2 \rangle}{I_m^2} = \exp[\sigma_\ell^2] - 1 = \sigma_\ell^2, \text{ for } \sigma_\ell^2 \ll 1. \quad (6)$$

To proceed, estimates of σ_ℓ^2 are needed. From Ref. 3 it can be shown that

$$\sigma_\ell^2 = 2.24 k^{7/6} (\sec\theta)^{11/6} \int_0^H C_n^2(h) h^{5/6} dh, \quad (7)$$

where θ is the zenith angle (for the case at hand $\theta < 60^\circ$), k is the optical wave number ($= 2\pi/\lambda$), H is the altitude of the receiver, and $C_n^2(h)$ is the index structure constant profile, i.e., the strength of turbulence as a function of height above ground. Because of the presence of the $h^{5/6}$ weighting function in the integrand of Eq. (7), σ_ℓ^2 is very insensitive to values of C_n^2 close to the ground. Rather, it is the high-altitude turbulence in the

tropopause at an altitude of about 9 to 12 km that is most effective in producing optical scintillation from a source on the ground.⁽¹⁾ Furthermore, for receiver altitudes H well above the turbulent atmosphere (i.e., $H \gg 20$ km), the value of the integral appearing in Eq. (7) is independent of H , from which it follows that the resulting log-irradiance variance does not depend on the altitude of the receiver.

On the basis of various empirical scintillation data, Hufnagel postulated that for optical and infrared wavelengths, the index of refraction structure constant for altitudes greater than 3 km above mean sea level is⁽¹⁾

$$C_n^2(h) = 2.72 \times 10^{-16} [3 V^2 \left(\frac{h}{10}\right)^{-10} e^{-h} + \exp(-h/1.5)] (m^{-2/3}), \quad (8)$$

where V^2 is the mean value of the wind speed squared in meters squared per seconds squared in the 5 to 20 km range, and h is the altitude in kilometers. Recent measurements have confirmed the approximate validity of this model. Barletti et al.⁴ measured C_n^2 at three different sites in Europe and found that for $h > 4$ km their results were nearly independent of site and agreed fairly well with the Hufnagel model. Vernin et al.⁵ measured C_n^2 at numerous sites in Italy, and again their results did not deviate greatly from the corresponding predicted values of the model. These measurements also indicated that there was very little seasonal variation in C_n^2 , the dominant quantity in all cases being the value of the root-mean-square wind speed V .

Substitution of Eq. (8) into Eq. (7) and performance of the integration yields

$$\sigma' = .41 \times 10^{-2} \left(\frac{V}{27}\right)^2 + 4.45 \times 10^{-3} \lambda^{-7/6} (\sec \theta)^{11/6}, \quad (9)$$

where λ is in units of μm . Figure 1 is a plot of Eq. (9) at $\lambda = 2.91 \mu\text{m}$ as a function of V for various values of θ . For example, at $\theta = 60^\circ$ and $V = 30 \text{ m/s}$, $\sigma_i^2 = 9.8 \times 10^{-2}$. In fact, for all cases of practical interest, ($V < 50 \text{ m/s}$) σ_i^2 , as measured above the earth's atmosphere and looking within zenith angles of less than 60° , σ_i^2 is always much less than unity.

In Table 1 the log-irradiance variance is given for various infrared wavelengths of interest for two representative root-mean-square wind speed values. The two values of V used represent, for the State of Maryland, the mean and one standard deviation above the mean value. As such, these cases should represent nominal and fairly strong turbulence conditions. Although larger values of V may be appropriate, they are relatively unlikely. In any event, if larger values of V are deemed operationally applicable, the corresponding numerical results can be obtained in a straightforward manner from the analytic results presented below.

Another quantity of interest is the covariance of normalized irradiance C_i , which is defined as

$$C_i(\underline{r}_1, \underline{r}_2) = \langle [i(\underline{r}_1, t) - i_m][i(\underline{r}_2, t) - i_m] \rangle. \quad (10)$$

Here \underline{r}_1 and \underline{r}_2 are two points in a plane perpendicular to the line of sight at the receiver altitude. Assuming the covariance of irradiance is stationary in the wide sense, it follows that $C_i(\underline{r}_1, \underline{r}_2) = C_i(\underline{r})$ where $\underline{r} = \underline{r}_1 - \underline{r}_2$. It can be shown that C_i is related to the corresponding covariance of log-irradiance C_ℓ as

$$C_i(\underline{r}) = \exp[C_\ell(\underline{r})] - 1 = C_\ell(\underline{r}), \text{ for } \sigma_\ell^2 \ll 1, \quad (11)$$

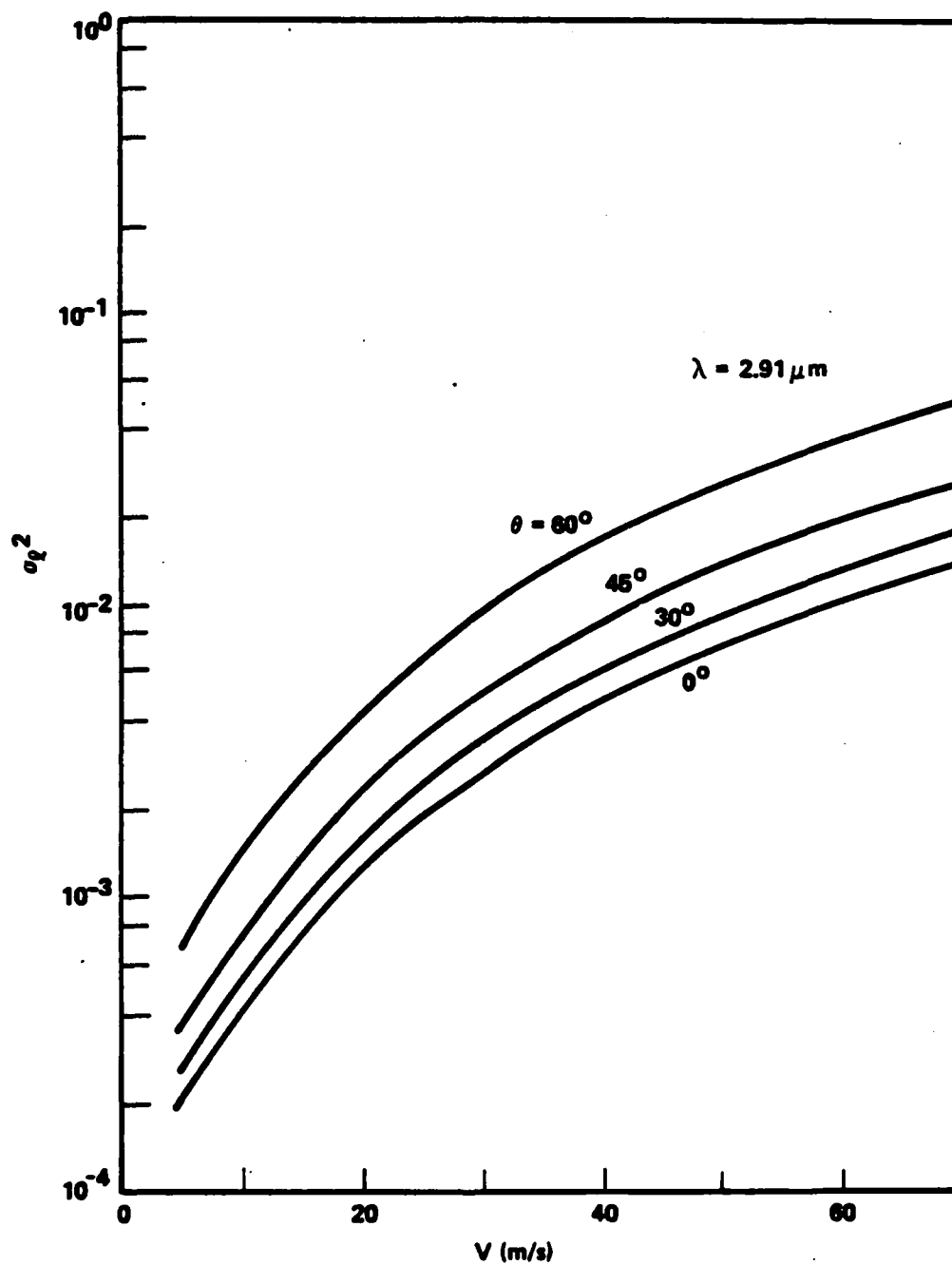


Fig. 1. Normalized log-irradiance variance as a function of root-mean-square wind speed V .

Table 1. Log-irradiance variance at several wavelengths for various values of the root-mean-square wind speed and zenith angles.

$\lambda(\mu\text{m})$	Log-irradiance variance σ_L^2			
	$\theta = 0^\circ$		$\theta = 60^\circ$	
	$V = 27 \text{ m/s}$	$V = 36 \text{ m/s}$	$V = 27 \text{ m/s}$	$V = 36 \text{ m/s}$
1.32	2.68×10^{-2}	9.85×10^{-2}	2.02×10^{-1}	3.51×10^{-1}
2.91	2.26×10^{-2}	3.91×10^{-2}	8.05×10^{-2}	1.40×10^{-1}
3.8	1.65×10^{-2}	2.87×10^{-2}	5.89×10^{-2}	1.02×10^{-1}
5.0	1.20×10^{-2}	2.08×10^{-2}	4.28×10^{-2}	7.42×10^{-2}
10.6	5.0×10^{-3}	8.66×10^{-3}	1.78×10^{-2}	3.09×10^{-2}

where

$$C_I(\underline{r}) = \langle [I(\underline{r}_1) - I_m][I(\underline{r}_2) - I_m] \rangle. \quad (12)$$

Note that $C_I(0) = \sigma_I^2$. Hence, we write $C_I(r) = \sigma_I^2 b_I(r)$, where $b_I(r)$ is the normalized irradiance correlation coefficient.

It can be shown that^(2,3)

$$b_I(r) = \frac{\int_0^H C_n^2(h) dh \int_0^\infty J_0[Kr(h/H)] \sin^2[K^2 h/2k] K^{-8/3} dK}{\int_0^H C_n^2(h) dh \int_0^\infty \sin^2[K^2 h/2k] K^{-8/3} dK}, \quad (13)$$

where J_0 is the zero-order Bessel function of the first kind. We do not dwell upon this quantity at any length except to note that the characteristic scale length r_I , defined as that value of r such that $b_I(r_I) = 0.5$ is, for the case at hand, of the order of

$$r_I \sim \left(\frac{H}{h_0}\right)(\lambda \Delta h)^{1/2},$$

where $h_0 = 10 - 12$ km, and $\Delta h \sim 3 - 5$ km. The precise values of h_0 and Δh depend weakly on V but are always in the range given above for all values of V of practical concern. Hence, in the infrared and for $H \gg 200$ km, $r_I \gg 1$ m, which is much larger than the receiver aperture assumed here. Thus, we can assume that the receiver is a "point" receiver, and no aperture averaging effects are expected.

III. TEMPORAL STATISTICS

The temporal changes in intensity are obtained from the assumption that the wind sweeps different turbulent eddies past the line of sight as a func-

tion of time. This is the "frozen in" model of turbulence and is justified for the present calculation. Of primary interest is the temporal power spectrum of irradiance or, equivalently, log-irradiance. As long as the log-irradiance variance is much less than unity, as it is in the present case, the irradiance power spectrum is equal to the log-irradiance power spectrum. For convenience, we present our results in terms of the log-irradiance power spectrum. The temporal power spectrum $P(f)$ is defined as the Fourier transform of the covariance function, and for the present case, it can be shown that⁽³⁾

$$P(f) = 8.27 (\sec\theta)^{7/3} k^{2/3} \int_0^H \frac{C_n^2(h) h^{4/3}}{v_n(h)} dh \quad (15)$$

$$\times \int_0^\infty \left[x^2 + \frac{f^2}{f_0^2(h)} \right]^{-11/6} \sin^2 \left[x^2 + f^2/f_0^2(h) \right] dx$$

where $v_n(h)$ is the wind speed normal to the direction of propagation at altitude h , and

$$f_0(h) = \left[\frac{2k}{h \sec\theta} \right]^{1/2} v_n(h) \quad (16)$$

Equation (15) has been integrated numerically for various cases of $v_n(h)$, obtained from simulated wind speed data, and the results are plotted in Figure 2 for various values of V , the root-mean-square wind speed, between 5 and 20 km. Examination of Figure 2 reveals that the bandwidth of the fluctuations are of the order of several hundred hertz for all cases of interest.

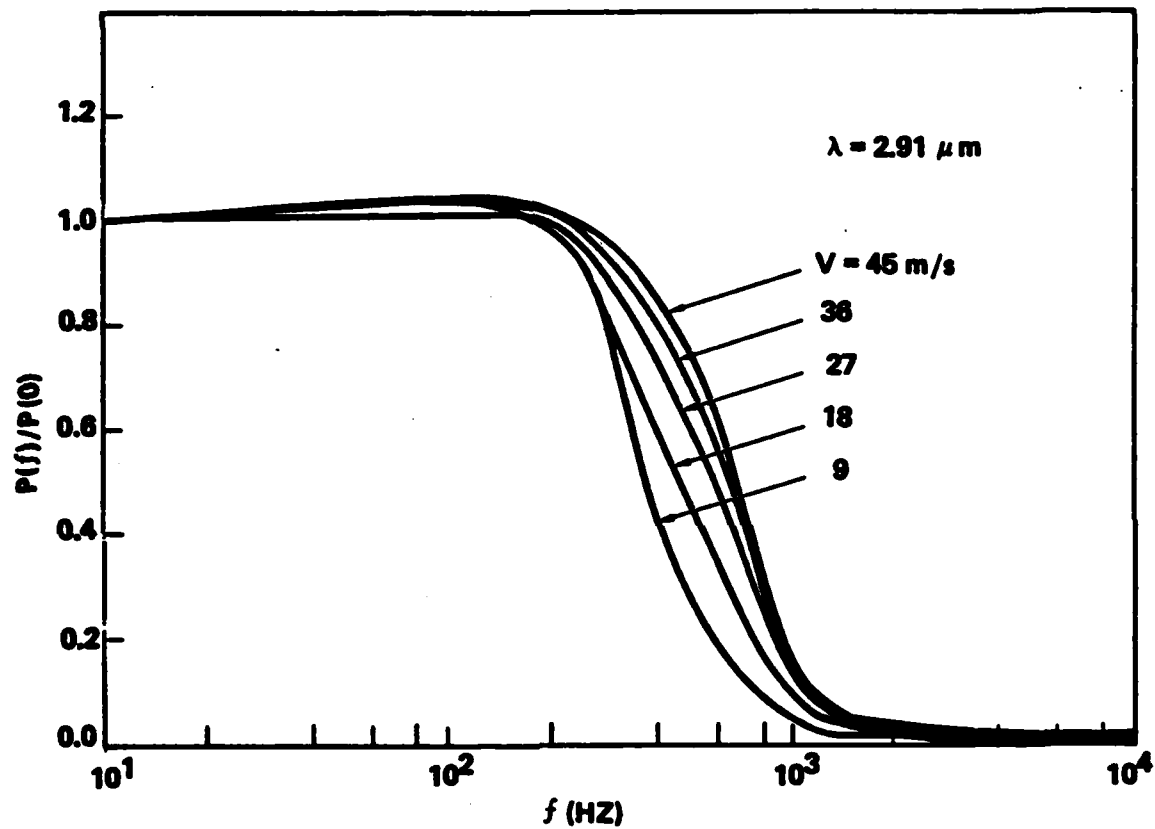


Fig. 2. Normalized irradiance temporal frequency spectrum for various values of V at $\lambda = 2.91 \mu\text{m}$.

IV. FADE AND SURGE STATISTICS

Next, the results for various probabilities of fades and surges are presented. In what follows, all irradiance values are assumed to be normalized to the mean value I_m . It is customary to refer to fades or surges in decibels. That is, if the value of irradiance is I , where I is greater (less) than I_m , then we are dealing with a surge (fade) of magnitude S dB, (F dB), where

$$S = 10 \log(I/I_m) \quad (17)$$

and

$$F = -10 |\log(I/I_m)| \quad (18)$$

The relationship between a given fade or surge level and the corresponding level of log-irradiance is obtained from Eqs. (1), (17), and (18) as

$$L_S = [\ln(10)/10] S = 0.23 S \text{ (Surges)} \quad (19a)$$

and

$$L_F = -[\ln(10)/10] F = -0.23 |F| \text{ (Fades)} \quad (19b)$$

We also present results for the following: (1) the fraction of time that the irradiance is above or below a given value, (2) the mean number of times per second that the irradiance crosses a given value, and (3) the mean duration of fade or a surge at a given level I . Again, we let $i(t)$ denote the instantaneous value of irradiance, normalized to its mean.

A. Fraction of Time of Fades and Surges

We obtain the fraction of time that $i(t) > i_0$ and $i(t) < i_0$, respectively. Since we are dealing with an ergodic process, where time averages are equal to ensemble averages, the fraction of time of a surge where $i > i_0$ [denoted by $\text{Frac}(i > i_0)$] is

$$\text{Frac}(i > i_0) = P_i(i > i_0) = P_l(l > l_0), \quad (20)$$

where P_i and P_l are the cumulative probabilities for irradiance and log-irradiance, respectively, and $i_0 = \exp(l_0)$. Similarly, the corresponding fraction of time of a fade $\text{Frac}(i < i_0)$ is

$$\text{Frac}(i < i_0) = P_i(i < i_0) = P_l(l < l_0). \quad (21)$$

Since l is normally distributed, we obtain

$$\begin{aligned} \text{Frac}(i < i_0) &= \frac{1}{(2\pi\sigma_l^2)^{1/2}} \int_{-\infty}^{l_{F_0}} \exp\left[-\frac{(l + 1/2 \sigma_l^2)^2}{2\sigma_l^2}\right] dl \\ &= \frac{1}{2} \left[1 + \text{erf}\left(\frac{l_{F_0} + (1/2)\sigma_l^2}{\sqrt{2} \sigma_l}\right)\right], \end{aligned} \quad (22)$$

where erf denotes the error function,

$$l_{F_0} = -0.23 F_0 \quad (23)$$

and F_0 is the fade level in decibels. Similarly, we obtain

$$\text{Frac}(i > i_0) = \frac{1}{2} [1 - \text{erf} \left\{ \frac{l_{S_0} + (1/2)\sigma_l^2}{\sqrt{2} \sigma_l} \right\}] \quad (24)$$

where

$$l_{S_0} = 0.23 S_0, \quad (25)$$

and S_0 is the surge level in decibels. Figures 3 and 4 are plots of Eqs. (22) and (24) as a function of σ_l^2 for various fade and surge levels.

B. Mean Frequency of Level Crossings

Another quantity of interest is the frequency of fades and surges. This is obviously identical to the frequency of positive or negative crossings of the level l_0 (i.e., $i_0 = I_0/I_m$), positive and negative referring to the slope of $l(t)$ at the time of crossing. We denote by $v^-(l_0)$ the mean frequency of negative crossings. As a result of symmetry, the mean frequency of positive crossings at level l_0 is also equal to $v^-(l_0)$. Since l is normally distributed with a mean equal to $-(1/2)\sigma_l^2$ and variance σ_l^2 , it can be shown⁽⁶⁾ that

$$v^-(l_0) = v_0 \exp \left[- \frac{[l_0 + (1/2)\sigma_l^2]^2}{2\sigma_l^2} \right] \quad (26)$$

where

$$v_0 = \left[\int_0^\infty f^2 P(f) df / \int_0^\infty P(f) df \right]^{1/2} \quad (27)$$

and $P(f)$ is the log-irradiance power spectrum. The quantity v_0 is referred to in the literature as the quasi-frequency.⁽⁶⁾ We numerically integrated Eq.

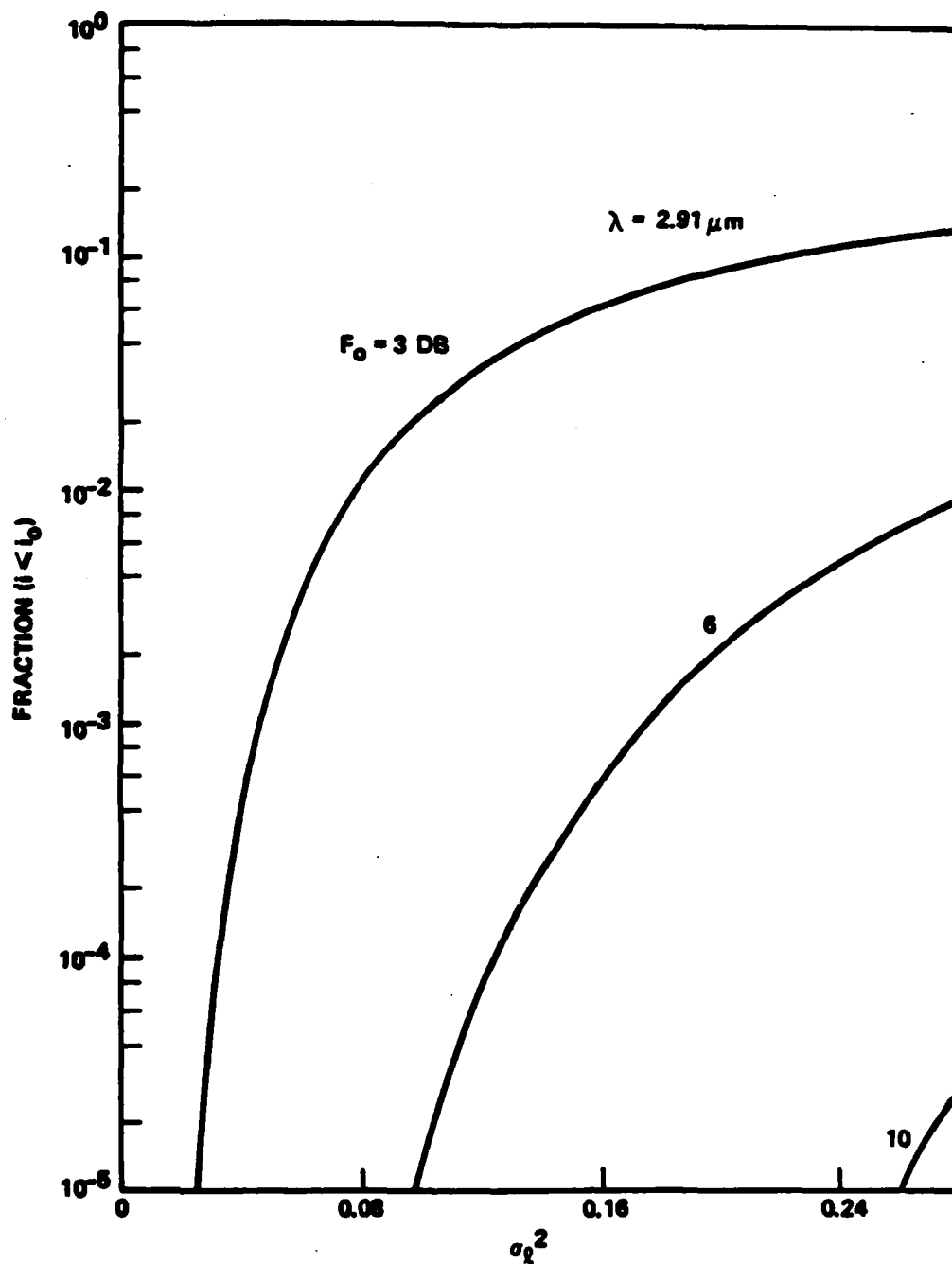


Fig. 3. Fraction of time that the irradiance is less than 3, 6, and 10 dB below the mean intensity.

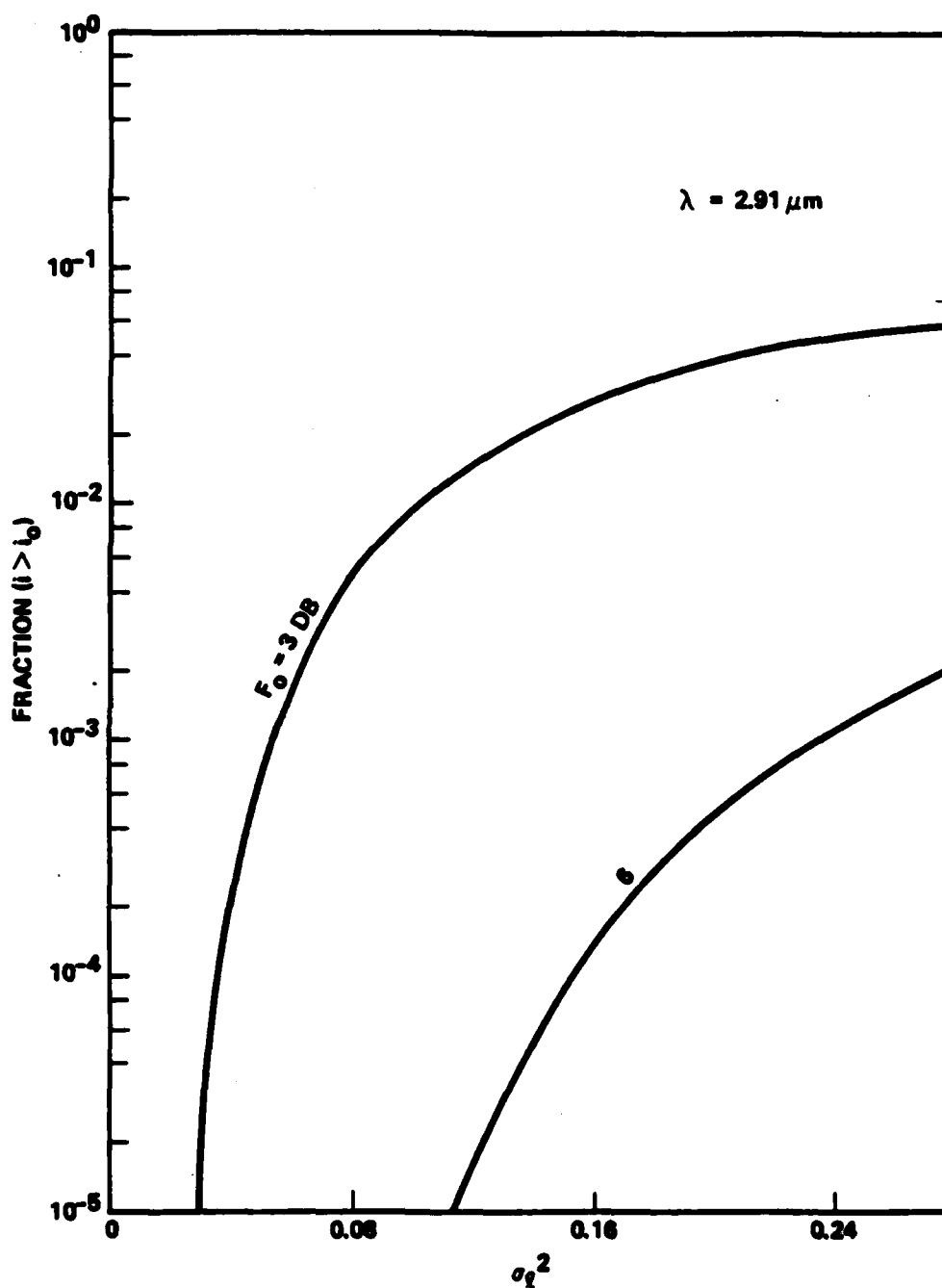


Fig. 4. Fraction of time that the irradiance is greater than 3 and 6 dB above the mean intensity level.

(27) and obtain that ν_0 is a relatively insensitive function of σ_L^2 for values of σ_L^2 of practical concern. We obtain that at $\lambda = 2.91 \mu\text{m}$, ν_0 is of the order 530 to 550 Hz over the range of interest. Hence, for a fade of F_0 dB, we obtain

$$\nu^-(F_0) = \nu_0 \exp \left[- \frac{[-0.23 F_0 + (1/2)\sigma_L^2]^2}{2\sigma_L^2} \right] \quad (28)$$

Similarly, for a surge of S_0 dB, we obtain that the mean frequency of positive crossings is

$$\nu^+(S_0) = \nu_0 \exp \left[- \frac{[0.23 S_0 + (1/2)\sigma_L^2]^2}{2\sigma_L^2} \right] \quad (29)$$

For example, Eq. (28) is plotted in Fig. 5 as a function of σ_L^2 for various fade values. Note that ν_0 is, strictly speaking, a function of σ_L^2 . However, as previously mentioned, it is a relatively insensitive function of σ_L^2 , and to obtain a worst-case estimate, we use the value of $\nu_0 = 550$ Hz at $\lambda = 2.91 \mu\text{m}$. Values of ν_0 at other wavelengths of interest can be obtained directly by noting that ν_0 is proportional to $\lambda^{-1/2}$.

In Figs. 6 and 7, we plot the mean level crossing frequency as a function of fade level for various wavelengths of interest in the infrared for zenith angles of 0 and 60°, respectively. In Fig. 8, we plot the level crossing frequency as a function of fade level for $\lambda = 1.32 \mu\text{m}$ and various values of the root-mean-square wind speed and zenith angles. An examination of Fig. 7, for example, reveals that the mean level crossing frequency associated with a 3 dB fade is about 70-75 Hz at 3.8 μm and a 60° zenith angle.

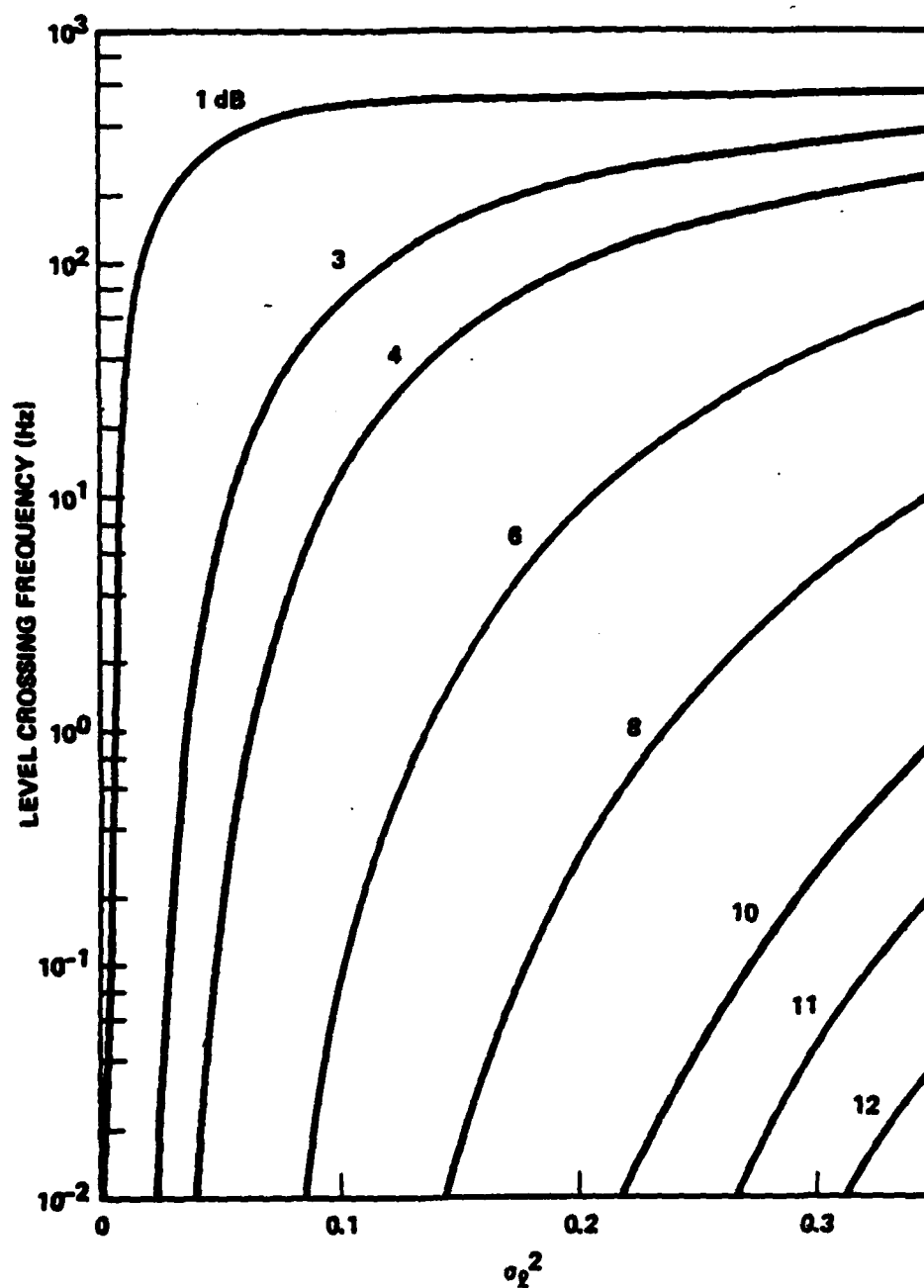


Fig. 5. Mean level crossing frequency as a function of normalized log-irradiance variance for various fade levels, $\lambda = 2.91 \mu\text{m}$.

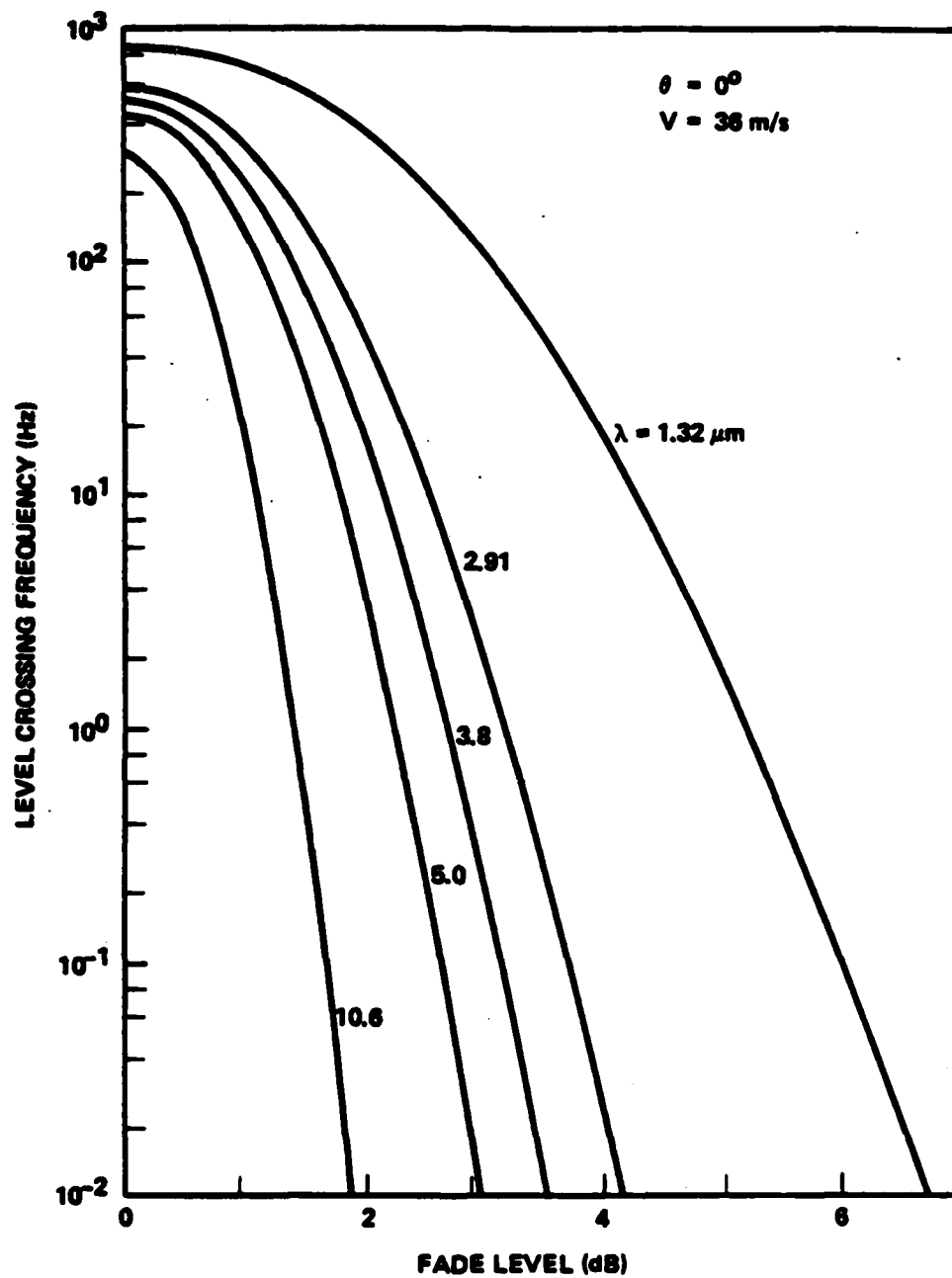


Fig. 6. Mean level crossing frequency as a function of fade level for various wavelengths: $V = 36 \text{ m/s}$, $\theta = 0^\circ$.

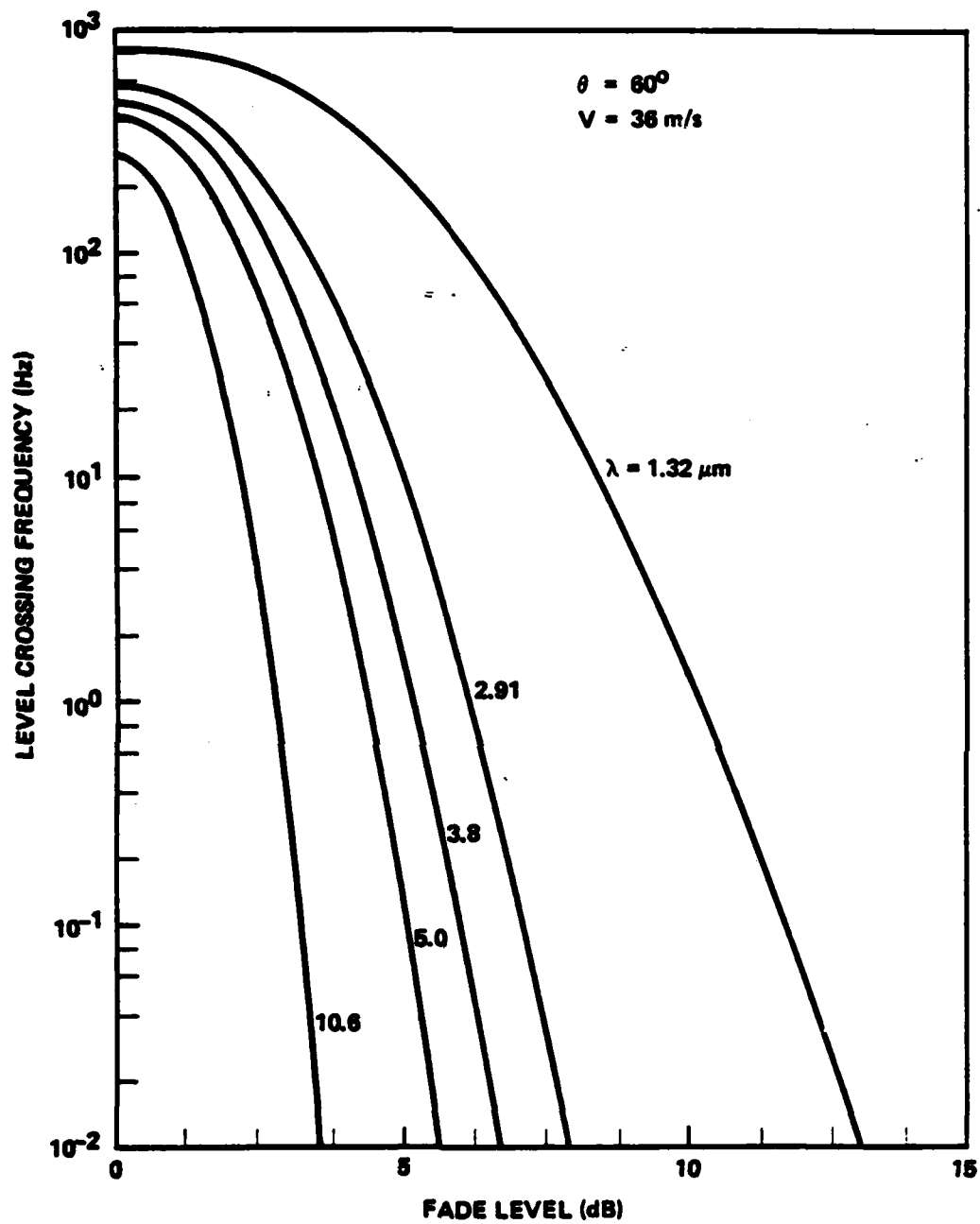


Fig. 7. Mean level crossing frequency as a function of fade level for various wavelengths: $V = 36 \text{ m/s}$, $\theta = 60^\circ$.

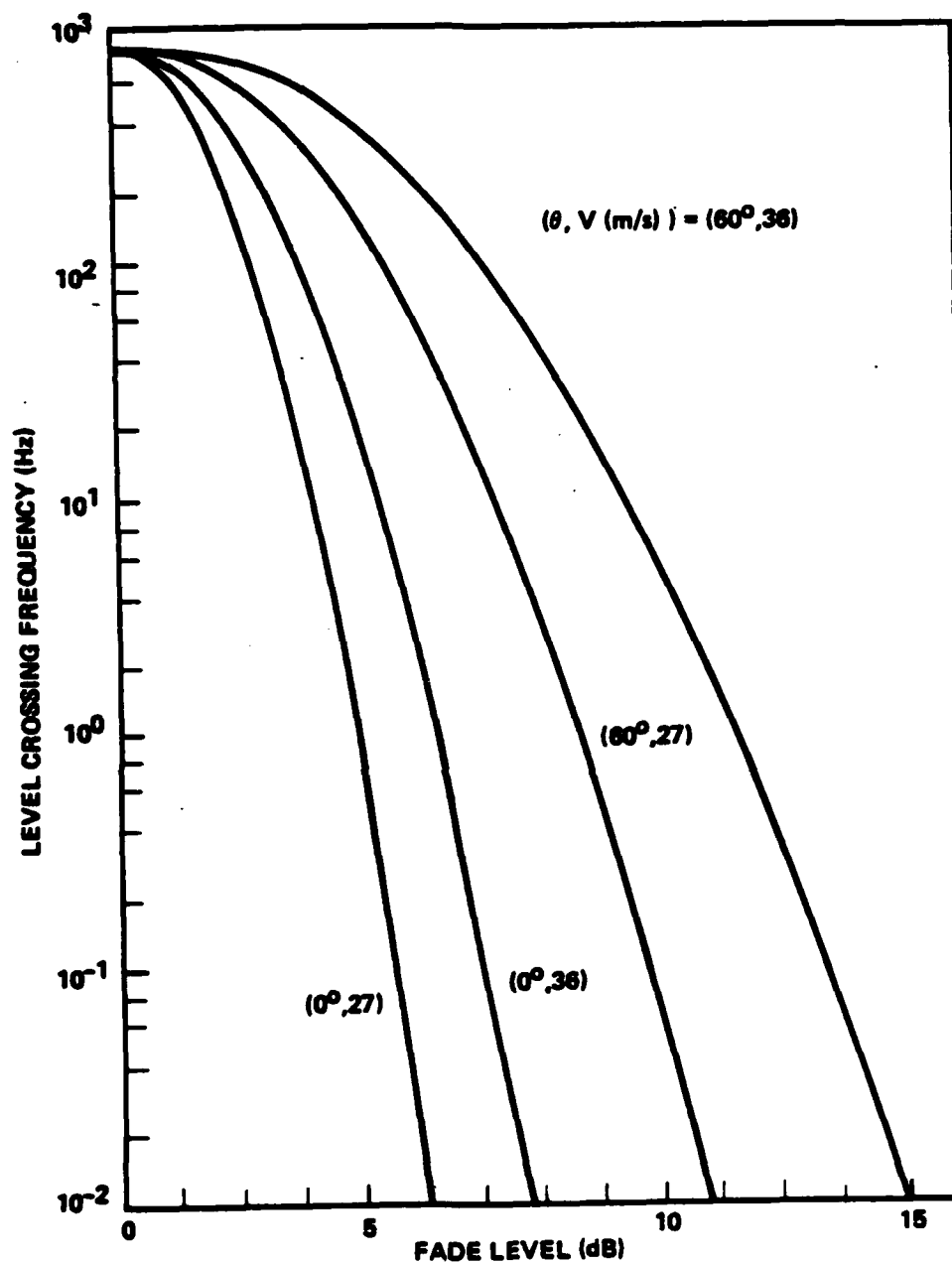


Fig. 8. Mean level crossing frequency at $\lambda = 1.32 \mu\text{m}$ for various root-mean-square wind speeds and zenith angles.

C. Mean Duration of Fades and Surges

The mean duration of a fade at level l_0 is

$$T^-(l_0) = \frac{P_l(l < l_0)}{v^-(l_0)}$$

$$= \frac{1}{2v_0} \exp\left[-\frac{[0.23 F_0 + (1/2)\sigma_l^2]^2}{2\sigma_l^2}\right] \left[1 + \operatorname{erf}\left\{\frac{[-0.23 F_0 + (1/2)\sigma_l^2]}{\sqrt{2}\sigma_l}\right\}\right] \quad (30)$$

and is plotted in Fig. 9 as a function of σ_l^2 . However, as previously mentioned, it is relatively insensitive function, and to obtain a worst-case estimate, we use the value $v_0 = 550$ Hz. Similarly, the mean duration of a surge at level l_0 is

$$T^+(l_0) = \frac{P_l(l > l_0)}{v^+(l_0)}$$

$$= \frac{1}{2v_0} \exp\left[-\frac{[0.23 S_0 + (1/2)\sigma_l^2]^2}{2\sigma_l^2}\right] \left[1 - \operatorname{erf}\left\{\frac{[0.23 S_0 + (1/2)\sigma_l^2]}{\sqrt{2}\sigma_l}\right\}\right]. \quad (31)$$

V. DISCUSSION

Statistical estimates of the communication parameters fade, surge, fade duration, surge duration, frequency of surge, and frequency of fade were derived for infrared laser ground-to-space communication systems operating in the 1 to 10 μm wavelength region. The equations are given in a form applicable for most atmospheric conditions of practical interest, e.g., a root-mean-square wind speed of 36 m/s, with $\lambda = 2.91 \mu\text{m}$ and a line-of-sight zenith angle of 60° . For these conditions, we obtain from Fig. 1 (or Table 1)

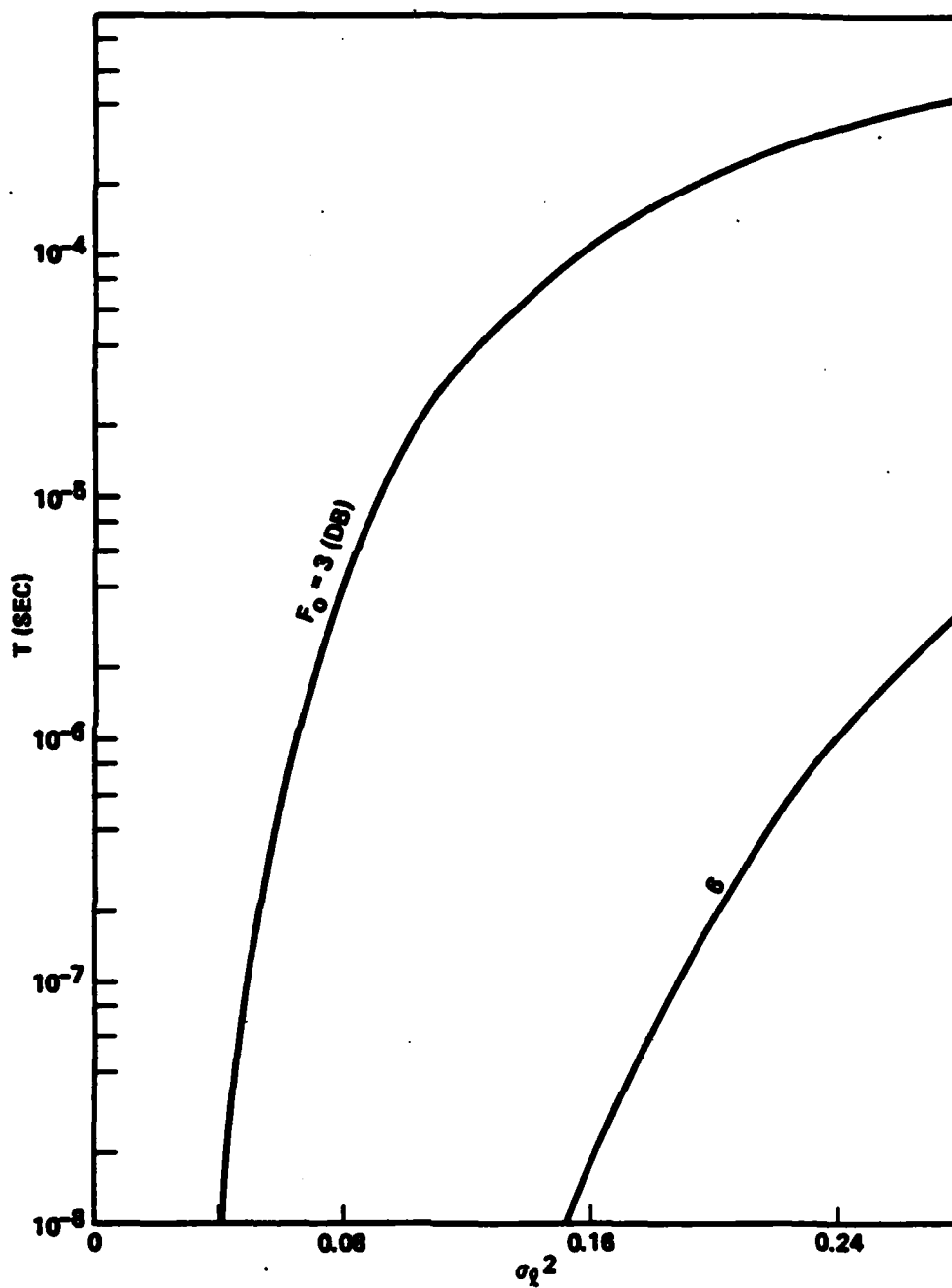


Fig. 9. Mean duration of 3 and 6 dB fades as a function of normalized log irradiance variance.

that $\sigma_I^2 = 0.14$. Once σ_I^2 is determined for the appropriate root-mean-square wind speed, we are then in a position to obtain the fade and surge statistics directly. We find from Fig. 3 that the fraction of time the irradiance is 3 dB below the mean intensity is ≈ 0.05 . Correspondingly, the mean frequency and duration of a 3 dB fade is, from Figs. 5 and 9, 150 Hz and 7×10^{-4} s, respectively. The statistics of other cases can be calculated with equal rapidity and, when used in conjunction with other information, enable one to estimate the availability of a given communication channel.

REFERENCES

1. R. E. Hufnagel, "Variation in Atmospheric Turbulence," Paper No. WA 1 in Digest of Technical Papers, Topical Meeting on Optical Propagation Through Turbulence, July 9-11, 1974, University of Colorado, Boulder, Colorado.
2. R. L. Fante, Proc. of the IEEE, 68, 1424 (1980).
3. V. I. Tatarskii, Wave Propagation in a Turbulent Medium, (McGraw Hill Book Co., New York, 1961).
4. R. Barletti, et al., J. Opt. Soc. Am. 66, 1380 (1976).
5. J. Vernin, et al., Appl. Opt. 18, 243 (1979).
6. P. Beckman, Probability in Communication and Engineering (Harcourt, Brace and World, Inc., New York, 1967), Chap. 6.

LABORATORY OPERATIONS

The Laboratory Operations of The Aerospace Corporation is conducting experimental and theoretical investigations necessary for the evaluation and application of scientific advances to new military space systems. Versatility and flexibility have been developed to a high degree by the laboratory personnel in dealing with the many problems encountered in the nation's rapidly developing space systems. Expertise in the latest scientific developments is vital to the accomplishment of tasks related to these problems. The laboratories that contribute to this research are:

Aerophysics Laboratory: Launch vehicle and reentry aerodynamics and heat transfer, propulsion chemistry and fluid mechanics, structural mechanics, flight dynamics; high-temperature thermomechanics, gas kinetics and radiation; research in environmental chemistry and contamination; cw and pulsed chemical laser development including chemical kinetics, spectroscopy, optical resonators and beam pointing, atmospheric propagation, laser effects and countermeasures.

Chemistry and Physics Laboratory: Atmospheric chemical reactions, atmospheric optics, light scattering, state-specific chemical reactions and radiation transport in rocket plumes, applied laser spectroscopy, laser chemistry, battery electrochemistry, space vacuum and radiation effects on materials, lubrication and surface phenomena, thermionic emission, photosensitive materials and detectors, atomic frequency standards, and bioenvironmental research and monitoring.

Electronics Research Laboratory: Microelectronics, GaAs low-noise and power devices, semiconductor lasers, electromagnetic and optical propagation phenomena, quantum electronics, laser communications, lidar, and electro-optics; communication sciences, applied electronics, semiconductor crystal and device physics, radiometric imaging; millimeter-wave and microwave technology.

Information Sciences Research Office: Program verification, program translation, performance-sensitive system design, distributed architectures for spaceborne computers, fault-tolerant computer systems, artificial intelligence, and microelectronics applications.

Materials Sciences Laboratory: Development of new materials: metal matrix composites, polymers, and new forms of carbon; component failure analysis and reliability; fracture mechanics and stress corrosion; evaluation of materials in space environment; materials performance in space transportation systems; analysis of systems vulnerability and survivability in enemy-induced environments.

Space Sciences Laboratory: Atmospheric and ionospheric physics, radiation from the atmosphere, density and composition of the upper atmosphere, aurorae and airglow; magnetospheric physics, cosmic rays, generation and propagation of plasma waves in the magnetosphere; solar physics, infrared astronomy; the effects of nuclear explosions, magnetic storms, and solar activity on the earth's atmosphere, ionosphere, and magnetosphere; the effects of optical, electromagnetic, and particulate radiations in space on space systems.

. . .

FILM

2-8

DTI